Available online at www.sciencedirect.com
SCIENCE DIRECT®
Composites Science and Technology 63 (2003) 1133–1139
COMPOSITES SCIENCE AND TECHNOLOGY
www.elsevier.com/locate/compscitech

Nano-porosity in silica reinforced methyltrimethoxysilane coatings studied by positron beam analysis

R. Escobar Galindo[a,*], A. van Veen[a], H. Schut[a], C.V. Falub[a], A.R. Balkenende[b], G. de With[c], J.Th.M. De Hosson[d]

[a]*Defects in Materials, Interfaculty Reactor Institute, Delft University of Technology, Mekelweg 15, NL-2629 JB Delft, The Netherlands*
[b]*Philips Research Laboratories, Prof. Holstlaan 4, NL-5656 AA, Eindhoven, The Netherlands*
[c]*Laboratory of Solid State and Materials Chemistry, Eindhoven University of Technology, NL-5600 MB Eindhoven, The Netherlands*
[d]*Materials Science Centre and NIMR, University of Groningen, Nijenborgh 4, NL-9747 AG Groningen, The Netherlands*

Abstract

The porosity in particle reinforced sol-gel coatings has been studied. Silica particles (Ludox-TM40) are introduced into methyl silicate coatings to increase the hardness, the elastic modulus and the fracture toughness. The methyl silicate has a relatively low density (about 1.2 g/cm^2), while the silica particles are known to be porous. However, the porosity of the silica particles is not accurately known. For model calculations on mechanical properties like the E-modulus this porosity should be known. Positron Beam Analysis (PBA), using the Doppler Broadening (DB) and 2D-Angular Correlation of Annihilation Radiation (2D-ACAR) techniques, was therefore performed for analysis of the porosity. Samples with different weight fractions (0, 20 and 63 wt.%) of silica particles of typically 40 nm in diameter and treated at different curing temperatures (623 and 723 K) were measured. With increasing filler content we observed a decrease in the positron annihilation *S*-parameter and a broadening of the para-positronium (p-Ps) fraction. By neglecting positron diffusion we can separate porosity in the matrix from that in the particles. This assumption is valid as long as the expected positron diffusion length is short compared to the size of the filler particles, as in the present case. A more detailed description takes into account the local environment of the filler particles affecting their adhesion to the matrix. It is concluded that the density of the silica particles is about 1.4 g/cm^2.

Keywords: A. Ceramic-matrix composites; A. Porosity; B. Mechanical properties; Positron beam analysis; E. Sol–gel methods

1. Introduction

The mechanical properties of sol-gel silicate coatings can be improved by introducing colloidal particles into the coating. With properly chosen particles, this leads to an increase of the critical thickness of the coatings, a reduction of residual stresses and to an increase of the fracture toughness [1].

In the present study, colloidal silica particles are introduced in methyl silicate ($SiO_{1.5}CH_3$) coating (obtained from methyltrimethoxysilane as a precursor) to increase the hardness, the elastic modulus and the fracture toughness. Micro-indentation and scratch testing [2] showed that the increase of the E-modulus with increasing particle content was significantly smaller than expected assuming a density of 2.2 g/cm^2. These results suggested that the particles might be porous, but also the introduction of voids into the matrix might play a role.

In order to obtain a more detailed structural analysis Positron Beam Analysis (PBA) using the Doppler Broadening (DB) and the 2D-Angular Correlation of Annihilation Radiation (2D-ACAR) techniques was performed. These techniques provide a non-destructive method to study open volume defects and porosity inside samples [3,4]. Positron techniques have been used quite recently to study composite systems [5,6]. Those studies use basically bulk positron lifetime measurements, but for the study of thin films the depth resolution that PBA provides is more convenient.

2. Experimental

The samples studied are methyltrimethoxysilane (MTMS)-derived coatings prepared via a sol-gel process

* Corresponding author. Tel.: +31-15-278-1612; fax. +31-15-278-6422.
E-mail address: rescobar@iri.tudelft.nl (R. Escobar Galindo).

0266-3538/03/$ - see front matter © 2003 Published by Elsevier Science Ltd.
doi:10.1016/S0266-3538(03)00034-4

and deposited on silicon substrates. Colloidal silica particles (Ludox-TM40), which have a diameter of approximately 40 nm, are mixed into the MTMS during the preparation of the coating solution. Then the solution is applied to the substrate via spin coating and subsequently cured at a temperatures of 623 or 723 K. Samples with varying weight fractions of silica particles (20 and 63 wt.%) were measured. In addition, a pure MTMS coating and a pressed pellet made from 100 nm sized Nyacol particles (similar to the Ludox filler particles) were measured as reference samples. The thickness of the coatings was 4 μm in the case of pure MTMS and 20 wt.% silica content samples and 2 μm for the 63 wt.% silica content samples.

The *Doppler broadening* (DB) experiments were performed with the Delft variable energy positron beam (VEP) [7]. The positrons were injected into the samples with energies tuned between 100 eV and 30 keV. The maximum implantation energy corresponds to a typical implantation depth of ~10 μm in low-density materials ($\rho \sim 1$ g/cm^3). All experiments were carried out at room temperature under a vacuum of about 10^{-6} Pa. PBA results are described in terms of two parameters. The S parameter indicates the fraction of positrons that annihilates with low momentum electrons (valence or conduction electrons). This parameter is related to the open volume defects present in the sample (e.g. pores). The W parameter indicates the fraction of positrons that annihilates with high momentum electrons (core electrons). This parameter is related to the chemical environment where the annihilation takes place. Both parameters can be combined in S–W maps where the different annihilation sites (layers) can be distinguished. The data was analysed with the VEPFIT [8] and SWAN [9] programs.

The *2D-ACAR* method [10] measures the deviation from the collinearity between the two annihilation photons. This deviation is of the order of a few milliradians. A high-intensity (10^8 e$^+$/s) tunable keV positron beam POSH, which employs a reactor based positron source, has been recently coupled to the 2D-ACAR target and detection system, enabling depth-selective studies in the (sub)-μm range. 2D-ACAR is a sensitive probe for resolving para-positronium (p-Ps) annihilation in nanoporous materials [11].

3. Results and discussion

3.1. Experimental observations

The results of DB experiments on the coatings are presented in Fig. 1 where the S and W parameters are shown as a function of the positron implantation depth. The positron implantation depth ($\bar{z}$) is derived, assuming a Makhovian implantation profile [12]:

$$\bar{z} = \frac{\alpha}{\rho} E^n \tag{1}$$

with $\alpha = 4.0$ μg/cm^2, $n = 1.62$, ρ is the density of the material and E the energy of the positrons in keV. In the case of the bulk Ludox pellet (*d*), only implantation energies up to 10 keV (~1μm) were probed. Those energies were sufficient to obtain a constant reference S and W values ($S_{\text{particles}} = 0.551$, $W_{\text{particles}} = 0.050$).

In Fig. 1a decrease of the S parameter and an increase of the W is observed with increasing the filler particles concentration (*a–d*). There is no difference observed in the positron behavior with the curing temperature.

The samples without filler particles presents constant values of S and W up to implantation depths of 4 μm corresponding to the layer thickness. The small oscillations observed in *a* are probably due to the presence of cracks in the sample. Beyond 4 μm implantation depth the S parameter decreases towards the value of the silicon substrate ($S_{\text{silicon}} = 0.578$). The W parameter first increases at 4 μm indicating the presence of the interface and then starts to decrease to the substrate value ($W_{\text{silicon}} = 0.029$). This is immediately evident from the S–W map of Fig. 2 where the cluster points from SWAN and VEPFIT analysis are included. This analysis will be described in Section 3.2.

The samples with 20 wt.% weight fraction of filler particles (*b*) presents a different behavior. In this case the S and W values are not constant throughout the layer thickness. In fact, the results indicate the presence of 2 regions inside the composite, both of about 2 μm thickness. VEPFIT analysis (Section 3.2) confirms this.

Finally the thinner sample (2μm) with 63 wt.% filler weight fraction shows again constant positron parameters through the coating. When positrons are implanted beyond the coating thickness, the S and W approach the silicon substrate cluster point.

2D-ACAR experiments were performed on the samples in order to obtained the fraction of para-positronium (p-Ps) created. The positron implantation depths indicated in Fig. 1 and Table 3 were used. A summary of the observations is presented in Table 3. In Fig. 3 a decrease in the central narrow part of the annihilation peak with the inclusion of filler particles is observed. This part is related to the formation of *p-Ps* and therefore to the porosity in the samples. Using the pure MTMS and the pressed pellet as reference, the porosity inside the composite samples can be studied. The analysis performed in Section 3.2 separates the porosity in terms of porosity inside the matrix and porosity inside the particles.

3.2. Analysis and modelling

The results of VEPFIT and SWAN analysis are summarized in Table 2 and plotted in Fig. 2. For simplicity

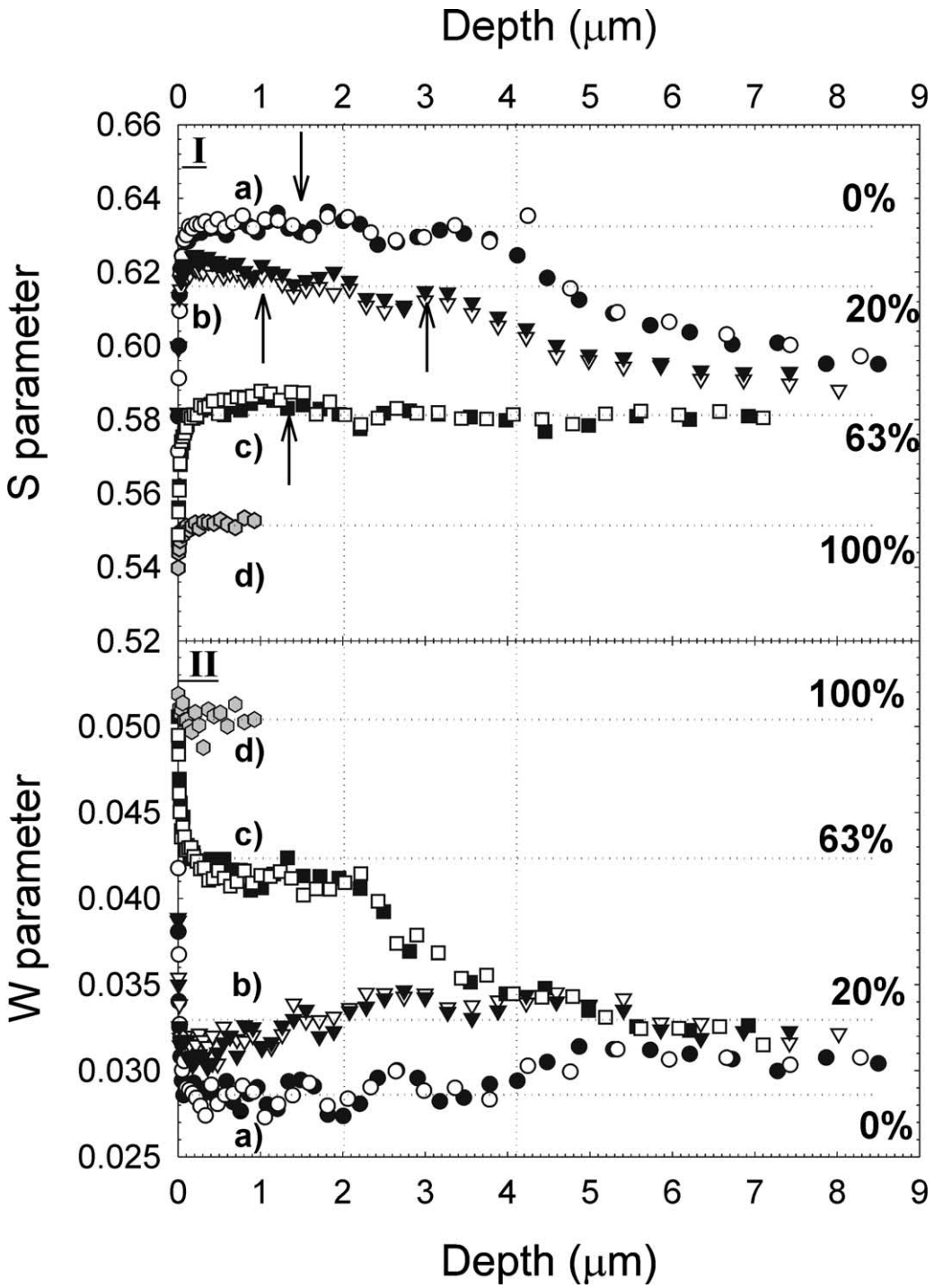

Fig. 1. Positron beam analysis experimental results: (I) *S*-parameter and (II) *W*-parameter versus positron implantation depth for the samples (a) 0 wt.%, b) 20 wt.%, (c) 63 wt.% and (d) 100 wt.% silica particles content. Closed symbols represent the samples cured at 623 K and open symbols represent the samples cured at 723 K. The vertical dotted lines indicate the thickness of the coatings (2 and 4 μm). The horizontal dotted lines indicate the *S* and *W* values obtained from the model. The arrows indicated the implantation depth were 2D-ACAR experiments were performed.

only the results of the analysis performed on the 623 K cured samples are shown. The results on the samples cured at 723 K were similar. A 4-layer system (surface, coating, interface and substrate) was used to simulate the three thin films. For the particle pellet (100 wt.%) only the surface and the bulk were included in the analysis.

The surface *S*–*W* cluster points (C.P.) of the unfilled and 20 wt.% filled samples are very similar (*a1, b1*), while the surface of highly filled sample (*c1*) resembles the one of the particle pellet sample (*d1*). Regarding the coating analysis, the most significant observation is the apparent presence of two stacked layers of ~2 μm each,

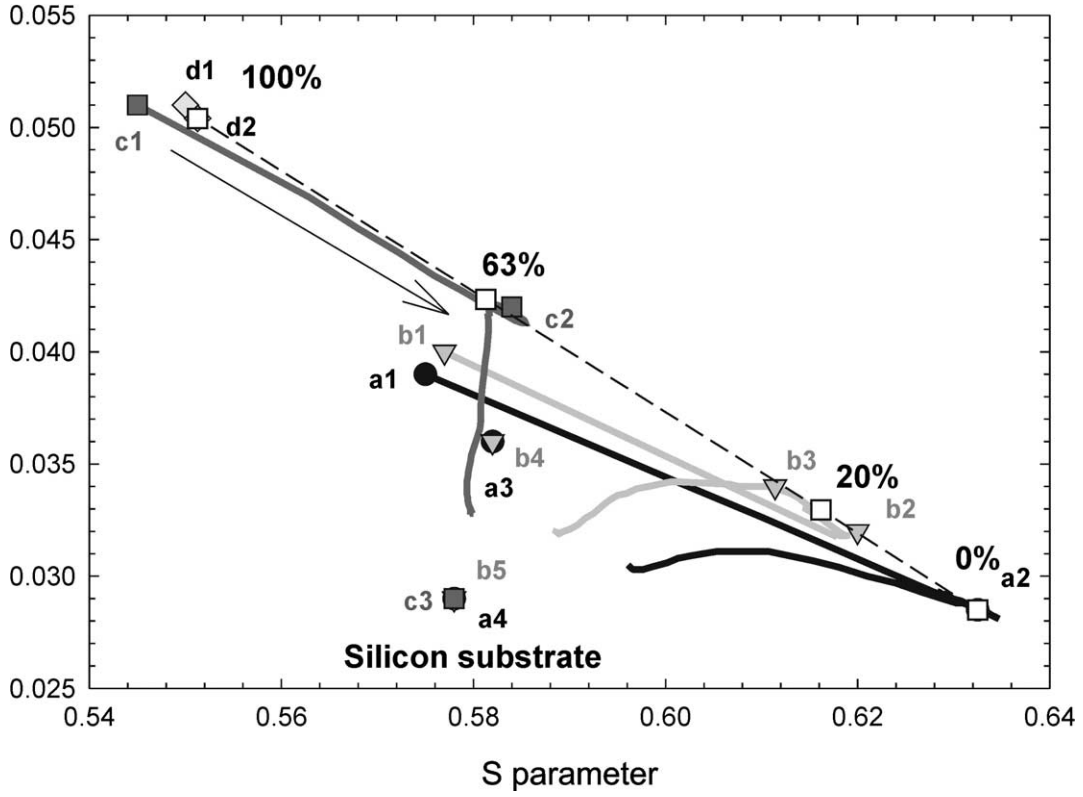

Fig. 2. *S–W* map comparing with the VEPFIT (closed symbols) and SWAN (continuous lines) analysis results with the model (open square and dashed line). The labels on the symbols correspond to the VEPFIT cluster points (C.P.) of the samples on Table 2. The error on *S* and *W* are represented by the size of the symbols. The arrow indicates the direction of increasing depth.

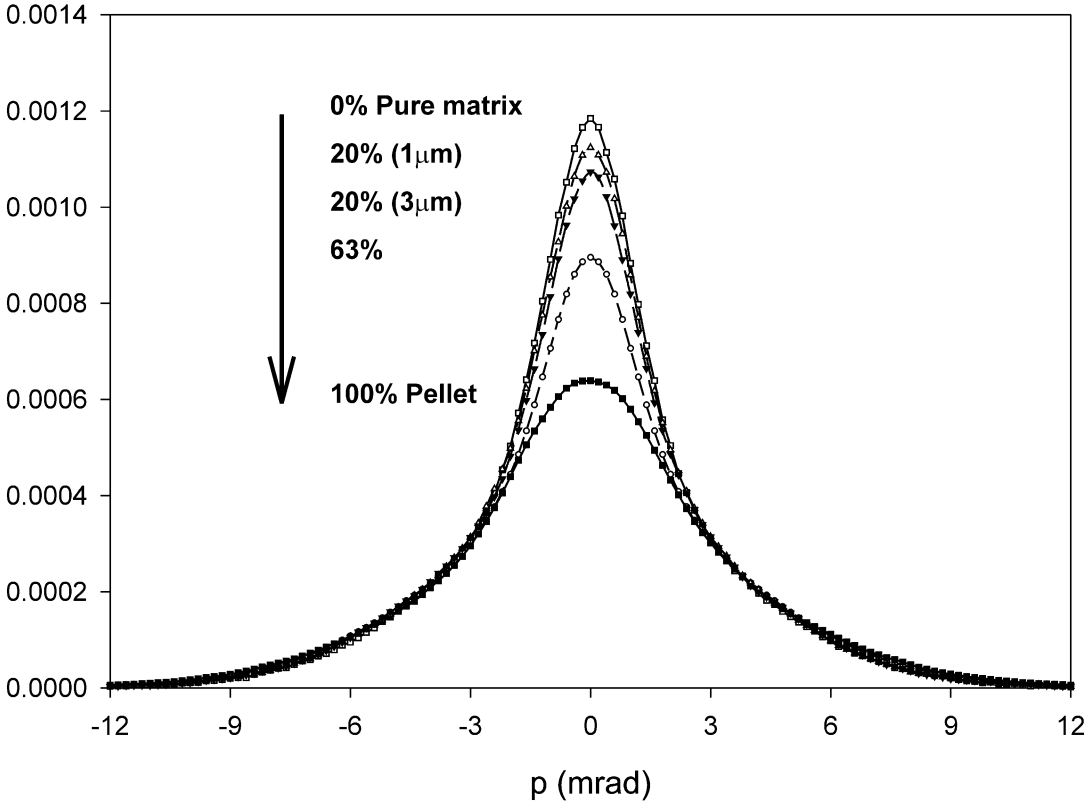

Fig. 3. 2D-ACAR cross sectional distributions of the samples studied. The 20% filled sample was studied for two different implantation depths (1 and 3 μm). The arrow indicates a decrease in the central part of the peak with increasing the filler content.

needed to describe the 20% filled sample. The cluster points *b2* and *b3* in Fig. 2 characterize those two layers. The cluster points associated with the different composite coatings (*a2, b2, b3* and *c2*) and with the bulk value of the particle pellet (*d2*) are on a straight line (see Fig. 2). Due to the linear nature of the S and W parameters this observation indicates that we can describe the S and W measured values (S_{exp}, W_{exp}) as a linear combination of annihilation in the matrix (characterized by S_{matrix}, W_{matrix} values) and in the silica particles ($S_{particles}$ and $W_{particles}$). This is allowed if we assume that the positron annihilates without diffusing after the implantation and thermalisation. It applies to our case, as the particle size (40 nm) is larger than the positron diffusion length inside the composite.

Then:

$$S_{exp} = f^{e^+}_{matrix} \times S_{matrix} + f^{e^+}_{particles} \times S_{particles} \quad (2a)$$

$$W_{exp} = f^{e^+}_{matrix} \times W_{matrix} + f^{e^+}_{particles} \times W_{particles} \quad (2b)$$

The fractions $f^{e^+}_{matrix}$ and $f^{e^+}_{particles}$ are the fraction of positrons annihilated in the matrix and in the filler particles, respectively. They are related to the volume particle content ($f^{vol}_{particles}$) and the density of each component in the following way:

$$f^{e^+}_{particles} = \frac{f^{vol}_{particles} \times \rho_{particles}}{f^{vol}_{particles} \times \rho_{particles} + (1 - f^{vol}_{particles}) \times \rho_{matrix}};$$
$$f^{e^+}_{matrix} = 1 - f^{e^+}_{particles} \quad (3)$$

Table 1
Description of the samples studied. The S_{model} and W_{model} were obtained considering the $f^{e^+}_{particles}$ equal to the $f^{wt}_{particles}$. In the last column $f^{e^+}_{particles}$ is obtained from experimental data

Sample	$f^{wt}_{particles}$ (wt.%)	Thickness (μm)	S_{model}	W_{model}	$f^{e^+}_{particles}$ (%)±5%
a	0	4	0.632	0.029	0
b	20	4	0.616	0.033	14.8
					24.7
c	63	2	0.581	0.042	59.3
d	100	Bulk	0.551	0.050	100

To take into account the different positron stopping factors of both components the volume the density weights fractions. Positrons are stopped more effectively in a denser material like the silica particles ($\rho_{particles}$ would be 1.53 g/cm^3 when we assume similar density for colloidal silica and for TEOS-derived sol-gel silica coatings) than in the methyl silicate matrix ($\rho_{matrix} = 1.17$ g/cm^3). This means that in our study $f^{e^+}_{particles}$ should be equal to $f^{wt}_{particles}$. Using the particle weight fractions from Table 1 we obtain S_{model} and W_{model} values to compare with the experimental data (see Table 1 and Fig. 2). We can also use the experimental S and W values and obtained then the $f^{e^+}_{particles}$ and compared it to the $f^{wt}_{particles}$ (see Table 1). It is observed that for the 20 wt.% filled sample the S–W point obtained from the model is in between the two cluster points (*b2* and *b3*) obtained from VEPFIT. This can be explained assuming a gradient of particle concentration (from ~15 wt.% near the surface to ~23 wt.%) over the coating thickness. For the 63 wt.% filled sample the model predicts a lower S value than measured. The positron fraction for this sample is 60%, that is, lower than the weight fraction. This might indicate a lower density for the particles than compared to the one found for sol-gel TEOS layers (1.53 g/cm^3). However, 2D-ACAR experiments should confirm this, as neglecting diffusion in our analysis might be an alternative cause for this disagreement.

The analysis of 2D-ACAR distributions is summarized in Table 3. The p-Ps component (narrow component) in the pure MTMS sample has a FWHM of 2.6±0.1 mrad and an intensity of 14±1% while in the particle pellet this component is broader (3.9±0.1 mrad) with an intensity of 15±1%. This indicates a smaller pore size inside the particles. Both samples have a broader component (8±0.1 mrad for the pure MTMS and 9.7±0.1 mrad for particle pellet) corresponding to positron annihilation in the bulk. The composite systems were analyzed using those four components (narrow-matrix, broad-matrix, narrow-particles and broad-particles), keeping constant the intensity ratio between the narrow and broad component of each reference sample. Doing so the p-Ps fraction can be separated into matrix and particles contributions.

In Fig. 4 it is observed that both the S-parameter and the p-Ps fraction inside the particles obtained from

Table 2
VEPFIT analysis results of the samples studied. The typical error in the S and W parameter affects the last significant digit. The cluster points (C.P.) columns refer to Fig. 2

$f^{wt}_{part.}$ (wt.%)	$S_{surf.}$	$W_{surf.}$	C.P.	$S_{coating}$	$W_{coating}$	C.P.	$S_{interf.}$	$W_{interf.}$	C.P.	$S_{silicon}$	$W_{silicon}$	C.P.
0	0.575	0.039	*a1*	0.632	0.029	*a2*	0.582	0.036	*a3*	0.578	0.029	*a4*
20	0.577	0.040	*b1*	0.620	0.032	*b2*	0.582	0.036	*b4*	0.578	0.029	*b5*
				0.612	0.034	*b3*						
63	0.545	0.545	*c1*	0.584	0.042	*c2*	–	–	–	0.578	0.029	*c3*
100	0.550	0.051	*d1*	0.551	0.050	*d2*	–	–	–	–	—	—

Table 3
2D-ACAR analysis results of the samples studied. The para-Positronium component has been decomposed in two terms regarding the particles and matrix contributions respectively. The $f^{Ps}_{particles}$ is defined as the ratio between the para-Positronium inside the particle and the total p-Ps

Sample	$f^{wt}_{particles}$ (wt.%)	Implantation depth(μm)	Total p-Ps (%)±1%	Matrix p-Ps (%)±1%	Particles p-Ps (%)±1%	$f^{Ps}_{particles}$ (%)±1%
a	0	1.6	14	14	0	0
b	20	1.0	16	12.5	3.5	23
		3.0	16	11.4	4.6	31
c	63	1.2	15.5	7	8.5	57
d	100	Bulk	15	0	15	100

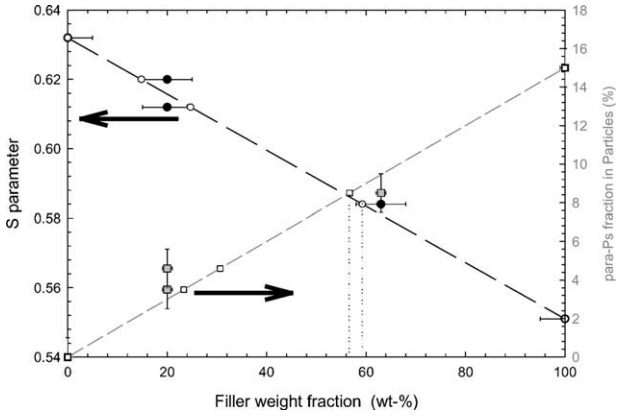

Fig. 4. *S* parameter (closed circles) and total Ps fraction (closed squares) are plotted versus the weight filer content of the samples. The dashed lines indicate the expected linear behaviour for both parameters. The open symbols (circles and squares) represent the weight filler content expected from the experimental data (DB and 2D-ACAR). The vertical dotted lines are to help the eye for the 63% sample. The error in the *S* parameter lies inside the closed circles.

2D-ACAR differ at high porosity from the expected linear behavior. There is a lower p-Ps contribution from the particles than expected. This is related to lower positron fraction annihilation (57±1%) than the weight fraction (63%) and confirms the DB results on a lower density of the particles. This density is estimated to be between 1.38±0.04 g/cm^3 (2D-ACAR) and 1.43±0.1 g/cm^3 (DB). At low porosity (20%) 2D-ACAR results confirms the existence of different particle content inside the coating although the fractions obtained are higher than the ones from DB.

As mentioned in Section 3.1 the presence of the coating-substrate interface is detected. This interface cluster point is about the same for the unfilled and 20 wt.% filled samples (*a3* and *b4*). This C.P. is relatively close to the surface values of both samples and therefore might be related to the presence of open volume or zones where the adhesion of the coating to the substrate is weak. The analysis of the highly filled sample did not reveal a cluster point associated with the coating-substrate interface. Looking at the *S*–*W* map of Fig. 2 it can be seen how the positron parameters change from the coating cluster point (*c2*) towards the silicon substrate (*c3*) almost in a straight line. This line passes through the interface cluster points ascribed to the unfilled and 20 wt.% filled samples. So it seems to be plausible that the interface between the composite coating and the silicon substrate can be described with the same positron cluster point regardless of the particle content.

4. Conclusions

Positron beam analysis has been performed for the first time on a particle reinforced system. A two-component model has been used to describe the positron parameters measured, revealing a gradient in composition for the 20 wt.% filled coating. At high filler content (63 wt.%) the para-Ps contribution inside the particles is lower than expected. This is attributed to a lower than expected density of the particles. This density was estimated to be 1.41±0.07 g/cm^3, compared to 1.53 g/cm^{-3} for sol-gel TEOS layers .The interface between the coating and the silicon substrate has been identified, and appears to have the same, relatively open, composition regardless of the particle content.

Acknowledgements

This work was financially supported by the Dutch Technology Foundation STW (project number GTF.4901).

References

[1] Shoup RD. Colloid Interf Sci 1976;3:63.
[2] Malzbender J, de Toonder JMJ, Balkenende AR, de With G. Mater Sci Eng 2002;R36:47–103.
[3] Nakanishi H, Jean YC. In: Schrader DM, Jean YC, editors. Positron and positronium chemistry, studies in physical and theoretical chemistry; vol. 57. Amsterdam: Elsevier; 1988. p. 159–92.
[4] van Veen A, Schut H, Mijnarends PE. In: Coleman P, editor. Positron beams and their applications. World Scientific Publishing Co.; 2000 [Chapter 6]..
[5] Flores KM, Suh D, Howell R, Asoka-Kumar P, Sterne PA, Dauskardt RH. Mater Trans 2001;42:619–22.
[6] Salgueiro W, Somoza A, Goyanes S, Rubiolo G, Marzocca A, Consolati G. Mater Sci Forum 2000;363-365:349–51.
[7] van Veen A, Trace J. Microprobe Techniques 1990;8:1–29.

[8] van Veen A, Schut H, de Vries J, Hakvoort RA, Ijpma MR. In: Schultz PJ, Massoumi GR, Simpson PJ, editors. AIP 218, Positron beams for solids and surfaces. 1990, p. 171–96.
[9] Fedorov AV, van Veen A, Schut H. Mater Sci Forum 2000;363-365:646–8.
[10] West RN. Positron spectroscopy of solids. In: Dupasquier A, Mills Jr AP, editors. Proc. Int. School of Physics "Enrico Fermi" Course CXXV. Amsterdam: IOS Press; 1995. p. 75–143.
[11] Gessmann Th, Petkov MP, Weber MH, Lynn KG, Rodbell KP, Asoka-Kumar P, Stoeffl W, Howell RH. Mater Sci Forum 2000; 363-365:585–7.
[12] Schultz PJ, Lynn KG. Rev Mod Phys 1989;60:701.